

November Clouds and the Earth's Radiant Energy System (CERES)

Algorithm Theoretical Basis Document

CERES Algorithm Overview

Bruce A. Wielicki, Interdisciplinary Principal Investigator¹

Bruce R. Barkstrom, Instrument Principal Investigator¹

¹Atmospheric Sciences Division, NASA Langley Research Center, Hampton, Virginia 23681-0001

Abstract

CERES (Clouds and the Earth's Radiant Energy System) is a key part of NASA's Earth Observing System (EOS). CERES objectives are

- 1. For climate change analysis, provide a continuation of the ERBE (Earth Radiation Budget Experiment) record of radiative fluxes at the top of the atmosphere (TOA) analyzed using the same techniques as the existing ERBE data.*
- 2. Double the accuracy of estimates of radiative fluxes at TOA and the Earth's surface.*
- 3. Provide the first long-term global estimates of the radiative fluxes within the Earth's atmosphere.*
- 4. Provide cloud property estimates which are consistent with the radiative fluxes from surface to TOA.*

These CERES data are critical for advancing the understanding of cloud-radiation interactions, in particular cloud feedback effects on the Earth's radiation balance. CERES data are fundamental to our ability to understand and detect global climate change. CERES results are also very important for studying regional climate changes associated with deforestation, desertification, anthropogenic aerosols, and El Niño events.

This overview summarizes the Release 2 version of the planned CERES data products and data analysis algorithms. These algorithms are a prototype for the system which will produce the scientific data required for studying the role of clouds and radiation in the Earth's climate system. This release will produce a data processing system to analyze the first CERES data planned for launch on TRMM in November 1997, followed by the EOS-AM platform in June 1998.

CERES Algorithm Theoretical Basis Document (ATBD)

Introduction

The purpose of this overview is to provide a brief summary of the CERES (Clouds and the Earth's Radiant Energy System) science objectives, historical perspective, algorithm design, and relationship to other EOS (Earth Observing System) instruments as well as important field experiments required for validation of the CERES results. The overview is designed for readers familiar with the ERBE (Earth Radiation Budget Experiment) and ISCCP (International Satellite Cloud Climatology Project) data. For other readers, additional information on these projects can be found in many references (Barkstrom 1984; Barkstrom and Smith 1986; Rossow et al. 1991; Rossow and Garder 1993). Given this background, many of the comments in this overview will introduce CERES concepts by comparison to the existing ERBE and ISCCP state-of-the-art global measurements of radiation budget and cloud properties. The overview will not be complete or exhaustive, but rather selective and illustrative. More complete descriptions are found in the ATBD's, and they are referenced where appropriate. The overview, as well as the entire set of ATBD's that constitute the CERES design are the product of the entire CERES Science Team and the CERES Data Management Team. We have simply summarized that work in this document.

Scientific Objectives

The scientific justification for the CERES measurements can be summarized by three assertions:

- Changes in the radiative energy balance of the Earth-atmosphere system can cause long-term climate changes (including a carbon dioxide induced “global warming”)
- Besides the systematic diurnal and seasonal cycles of solar insolation, changes in cloud properties (amount, height, optical thickness) cause the largest changes of the Earth’s radiative energy balance
- Cloud physics is one of the weakest components of current climate models used to predict potential global climate change

The international assessment of the confidence in predictions using global climate models (IPCC 1992) concluded that “the radiative effects of clouds and related processes continue to be the major source of uncertainty.” The U.S. Global Change Research Program classified the role of clouds and radiation as its highest scientific priority (CEES, 1994). There are many excellent summaries of the scientific issues (Climate Change, 1995;; Hansen et al. 1993; Ramanathan et al. 1989; Randall et al. 1989; Wielicki et al. 1995) concerning the role of clouds and radiation in the climate system. These issues naturally lead to a requirement for improved global observations of both radiative fluxes and cloud physical properties. The CERES Science Team, in conjunction with the EOS Investigators Working Group representing a wide range of scientific disciplines from oceans, to land processes, to atmosphere, has examined these issues and proposed an observational system with the following objectives:

- For climate change analysis, provide a continuation of the ERBE record of radiative fluxes at the TOA, analyzed using the same algorithms that produced the existing ERBE data
- Double the accuracy of estimates of radiative fluxes at the TOA and Earth’s surface
- Provide the first long-term global estimates of the radiative fluxes within the Earth’s atmosphere
- Provide cloud property estimates which are consistent with the radiative fluxes from surface to TOA

The most recent IPCC assessment of climate change (Climate Change, 1995) concludes that the remaining uncertainties include “feedbacks associated with clouds” and “systematic collection of long-term instrumental and proxy observations of the climate system variables (e.g., solar output, atmospheric energy balance components, . . .” The long-term CERES measurements target both of these needs.

The CERES Algorithm Theoretical Basis Documents (ATBD’s) provide a technical plan for accomplishing these scientific objectives. The ATBD’s include detailed specification of data products, as well as the algorithms used to produce those products. CERES validation plans are provided in a separate set of documents.

Historical Perspective

We will briefly outline the CERES planned capabilities and improvements by comparison to the existing ERBE, ISCCP, and SRB (Surface Radiation Budget) projects. Figure 1 shows a schematic of radiative fluxes and cloud properties as produced by ERBE, SRB, and ISCCP, as well as those planned for CERES. Key changes are listed below:

Scene Identification

- ERBE measured only TOA fluxes and used only ERBE radiance data, even for the difficult task of identifying each ERBE field of view (FOV) as cloudy or clear.
- CERES will identify clouds using collocated high spectral and spatial resolution cloud imager radiance data from the same spacecraft as the CERES broadband radiance data, (ATBD subsystem 4).
- ERBE only estimated cloud properties as one of four cloud amount classes.
- CERES will identify clouds by cloud amount, height, optical depth, and cloud particle size and phase.

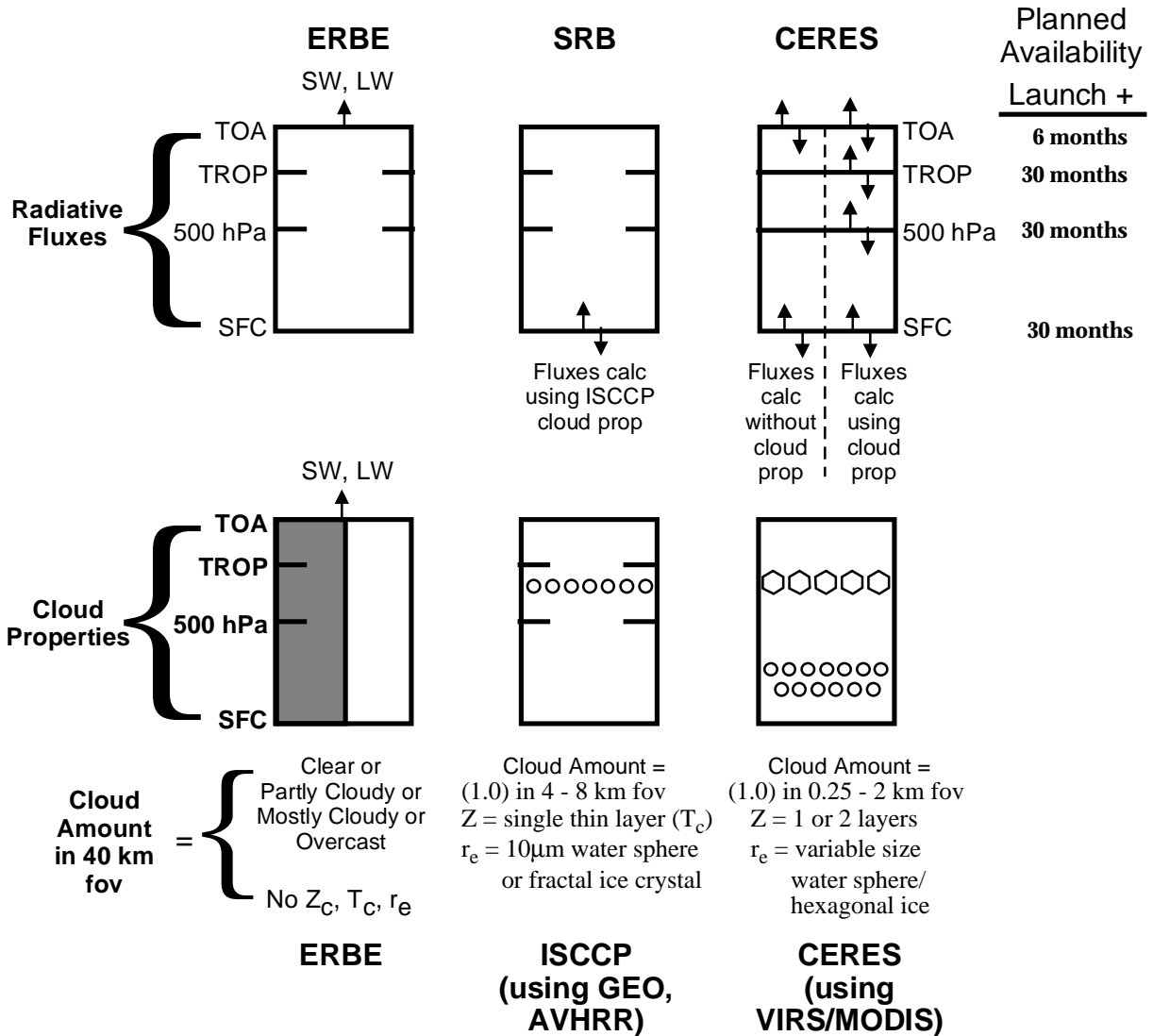


Figure 1. The top of the figure compares radiative fluxes derived by ERBE, SRB, and CERES. The bottom compares cloud amount and layering assumptions used by ERBE, ISCCP, and CERES.

Angular Sampling

- ERBE used empirical anisotropic models which were only a function of cloud amount and four surface types (Wielicki and Green 1989). This caused significant rms and bias errors in TOA fluxes (Suttles et al. 1992).
- CERES will fly a new rotating azimuth plane (RAP) scanner to sample radiation across the entire hemisphere of scattered and emitted broadband radiation. The CERES RAP scanner data will be merged with coincident cloud imager derived cloud physical and radiative properties to develop a more complete set of models of the radiative anisotropy of shortwave (SW) and long-wave (LW) radiation. Greatly improved TOA fluxes will be obtained.

Time Sampling

- ERBE used a time averaging strategy which relied only on the broadband ERBE data and used other data sources only for validation and regional case studies.

- CERES will use the 3-hourly geostationary satellite data of ISCCP to aid in time interpolation of TOA fluxes between CERES observation times. Calibration problems with the narrowband ISCCP data will be eliminated by adjusting the data to agree at the CERES observation times. In this sense, the narrowband data are used to provide a diurnal cycle perturbation to the mean radiation fields.

Surface and In-Atmosphere Radiative Fluxes

- SRB uses ISCCP-determined cloud properties and calibration to estimate surface fluxes.
- CERES will provide two types of surface fluxes: *first*, a set which attempts to directly relate CERES TOA fluxes to surface fluxes; *second*, a set which uses the best information on cloud, surface, and atmosphere properties to calculate surface, in-atmosphere, and TOA radiative fluxes, and then constrains the radiative model solution to agree with CERES TOA flux observations.
- Radiative fluxes within the atmosphere will initially be provided at the tropopause and at selected levels in the stratosphere (launch plus 30 months). Additional radiative flux estimates at 500 hPa (launch + 30 months) and at 4-12 additional levels in the troposphere (launch + 42 months) are planned, with the number of tropospheric levels dependent on the results of post-launch validation studies.

CERES Algorithm Summary

Data Flow Diagram

The simplest way to understand the structure of the CERES data analysis algorithms is to examine the CERES data flow diagram shown in figure 2. Circles in the diagram represent algorithm processes which are formally called subsystems. Subsystems are a logical collection of algorithms which together convert input data products into output data products. Boxes represent archival data products. Boxes with arrows entering a circle are input data sources for the subsystem, while boxes with arrows exiting the circles are output data products. Data output from the subsystems falls into three major types of archival products:

1. **ERBE-like Products** which are as identical as possible to those produced by ERBE. These products are used for climate monitoring and climate change studies when comparing directly to ERBE data sources (process circles and ATBD subsystems 1, 2, and 3).
2. **SURFACE Products** which use cloud imager data for scene classification and new CERES-derived angular models to provide TOA fluxes with improved accuracy over those provided by the ERBE-like products. Second, direct relationships between surface fluxes and TOA fluxes are used where possible to construct SRB estimates which are as independent as possible of radiative transfer model assumptions, and which can be tuned directly to surface radiation measurements. These products are used for studies of land and ocean surface energy budget, as well as climate studies which require higher accuracy TOA fluxes than provided by the ERBE-like products (process circles and ATBD subsystems 1, 4, 9, and 10).
3. **ATMOSPHERE Products** which use cloud-imager-derived cloud physical properties, NCEP (National Centers for Environmental Prediction) or EOS DAO (Data Assimilation Office) temperature and moisture fields, ozone and aerosol data, CERES observed surface properties, and a broadband radiative transfer model to compute estimates of SW and LW radiative fluxes (up and down) at the surface, at levels within the atmosphere, and at the TOA. By adjusting the most uncertain surface and cloud properties, the calculations are constrained to agree with the CERES TOA-measured fluxes, thereby producing an internally consistent data set of radiative fluxes and cloud properties. These products are designed for studies of energy balance within the atmosphere, as well as climate studies which require consistent cloud, TOA, and surface radiation data sets.

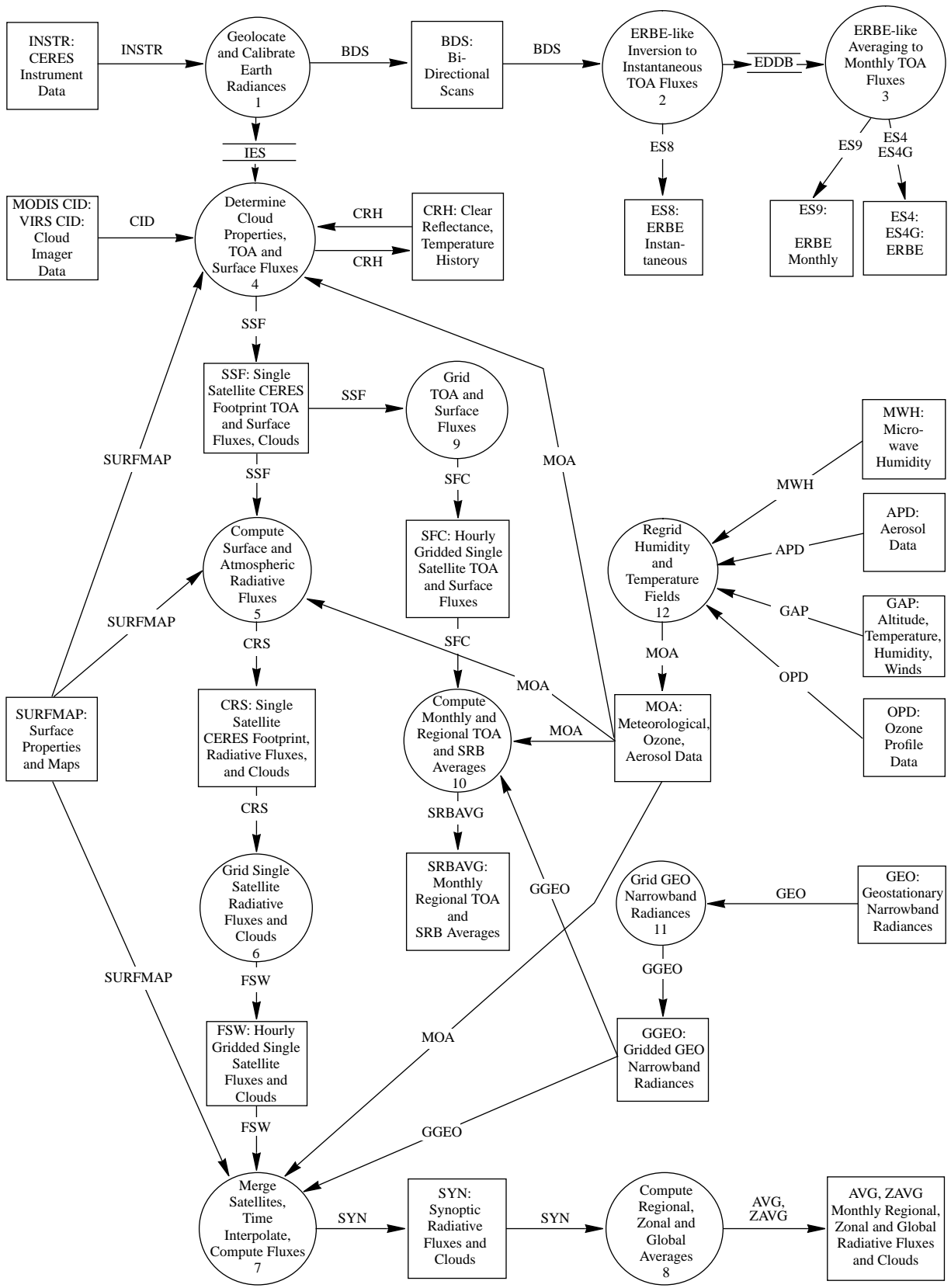


Figure 2. The CERES data flow diagram. Boxes represent input or output archived data products. The circles represent algorithm processes.

Data volume is much larger than ERBE-like or Surface products (process circles and ATBD subsystems 1, 4, 5, 6, 7, and 8).

The data flow diagram and the associated ATBD's are a work in progress. They represent the current understanding of the CERES Science Team and the CERES Data Management Team. The ATBD's are meant to change with time. To manage this evolution, the data products and algorithms will be developed in four releases or versions.

Release 1 (1996) is the initial prototype system. Release 1 is sufficiently complete to allow testing on existing global satellite data from ERBE, AVHRR (Advanced Very High Resolution Radiometer), and HIRS (High-Resolution Infrared Sounder) instruments for October 1986 on NOAA-9. This release provides estimates of the computational resources required to process the CERES data, as well as sensitivity studies of initial algorithm performance for global conditions.

Release 2 (1997) is the first operational system. It will be designed using the experience from Release 1, and will be ready to process the first CERES data following the planned launch of the Tropical Rainfall Measuring Mission (TRMM) in November 1997, as well as the first CERES data from the EOS-AM platform planned for launch in June 1998.

Release 3 (1998) adds the capability to analyze MODIS radiance data to provide cloud properties. Release 3 will be used to process initial EOS-AM and EOS-PM data.

Release 4 (2001) is planned for 3 years after the launch of the EOS-AM platform. Release 4 improvements will include new models of the anisotropy of SW and LW radiation (subsystem 4.5) using the CERES RAP scanner (subsystem 1.0) and additional vertical levels of radiative fluxes within the atmosphere (subsystem 5.0). Note that Release 4 will require a reprocessing of the earlier Release 2 and 3 data to provide a time-consistent climate data set for the CERES observations.

The following sections will give a brief summary of the algorithms used in each of the subsystems shown in figure 2. For more complete descriptions, the ATBD's are numbered by the same subsystem numbers used below.

Subsystem 1: Instrument Geolocate and Calibrate Earth Radiances

The instrument subsystem converts the raw, level 0 CERES digital count data into geolocated and calibrated filtered radiances for three spectral channels: a total channel (0.3–200 μm), a shortwave channel (0.3–5 μm), and a longwave window channel (8–12 μm) (Lee et al. 1996). Details of the conversion, including ground and on-board calibration can be found in ATBD subsystem 1. The CERES scanners are based on the successful ERBE design, with the following modifications to improve the data:

- Improved ground and onboard calibration by a factor of 2. The accuracy goal is 1% for SW and 0.5% for LW.
- Angular FOV reduced by a factor of 2 to about 20 km at nadir for EOS-AM orbit altitude of 700 km. This change is made to increase the frequency of clear-sky and single-layer cloud observations, as well as to allow better angular resolution in the CERES derived angular distribution models (ADM's), especially for large viewing zenith angles.
- Improved electronics to reduce the magnitude of the ERBE offsets.
- Improved spectral flatness in the broadband SW channel.
- Replacement of the ERBE LW channel (nonflat spectral response) with an 8–12- μm spectral response window.

The CERES instruments are designed so that they can easily operate in pairs as shown in figure 3. In this operation, one of the instruments operates in a fixed azimuth crosstrack scan (CTS) which optimizes spatial sampling over the globe. The second instrument (RAP scanner) rotates its azimuth plane

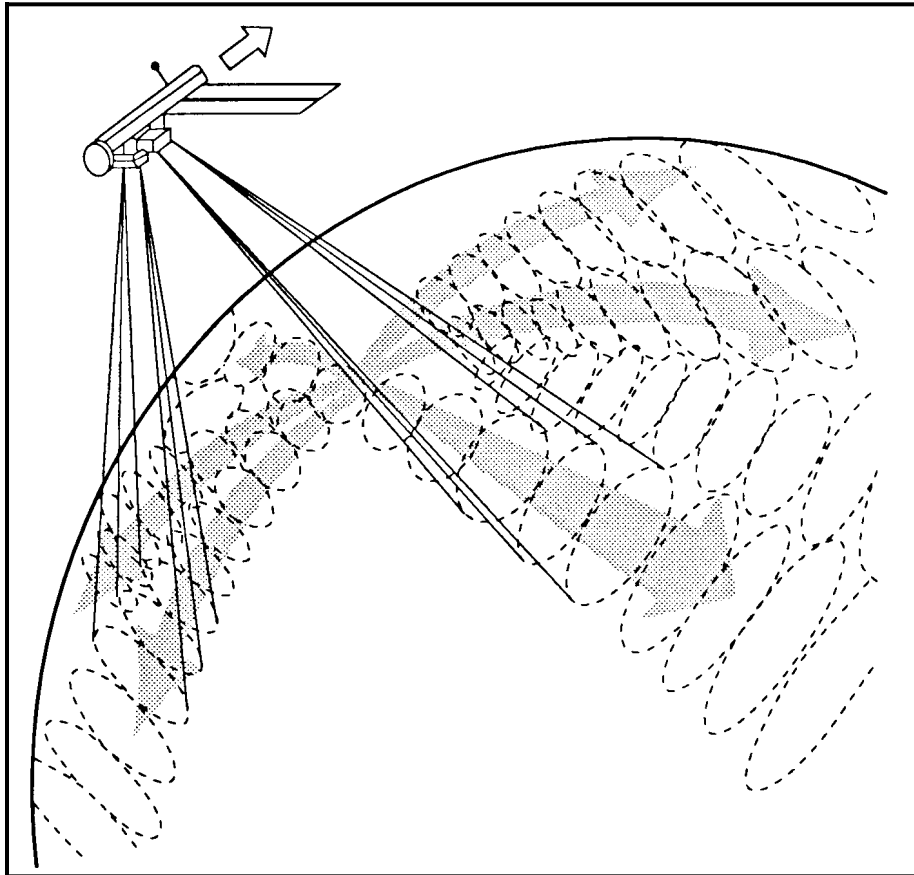


Figure 3. The scan pattern of two CERES scanners on EOS-AM and EOS-PM spacecraft. One scanner is cross-track, the other scanner rotates in azimuth angle as it scans in elevation, thereby sampling the entire hemisphere of radiation.

scan as it scans in elevation angle, thereby providing angular sampling of the entire hemisphere of radiation. The RAP scanner, when combined with cloud imager classification of cloud and surface types, will be used to provide improvements over the ERBE ADM's (ATBD subsystem 4.5). Each CERES instrument is identical, so either instrument can operate in either the CTS or RAP scan mode. An initial set of 6 CERES instruments is being built, including deployment on:

- TRMM (1 scanner), 35-degree inclined processing orbit, launch November 1997
- EOS-AM (2 scanners), 10:30 a.m. sun-synchronous orbit, launch June 1998
- EOS-PM (2 scanners), 1:30 p.m. sun-synchronous orbit, launch January 2000
- TRMM follow on, 57-degree precessing orbit 2002 (not yet confirmed)

Subsystem 2: ERBE-Like Inversion to Instantaneous TOA Fluxes

The ERBE-like inversion subsystem converts filtered CERES radiance measurements to instantaneous radiative flux estimates at the TOA for each CERES field of view. The basis for this subsystem is the ERBE Data Management System which produced TOA fluxes from the ERBE scanning radiometers onboard the ERBS (Earth Radiation Budget Satellite), NOAA-9 and NOAA-10 satellites over a 5-year period from November 1984 to February 1990 (Barkstrom 1984; Barkstrom and Smith 1986). The ERBE Inversion Subsystem (Smith et al. 1986) is a mature set of algorithms that has been well documented and tested. The strategy for the CERES ERBE-like products is to process the data through the

same algorithms as those used by ERBE, with only minimal changes, such as those necessary to adapt to the CERES instrument characteristics.

Subsystem 3: ERBE-Like Averaging to Monthly TOA

This subsystem temporally interpolates the instantaneous CERES flux estimates to compute ERBE-like averages of TOA radiative parameters. CERES observations of SW and LW flux are time averaged using a data interpolation method similar to that employed by the ERBE Data Management System. The averaging process accounts for the solar zenith angle dependence of albedo during daylight hours, as well as the systematic diurnal cycles of LW radiation over land surfaces (Brooks et al. 1986).

The averaging algorithms produce daily, monthly-hourly, and monthly means of TOA and surface SW and LW flux on regional, zonal, and global spatial scales. Separate calculations are performed for clear-sky and total-sky fluxes.

Subsystem 4: Overview of Cloud Retrieval and Radiative Flux Inversion

One of the major advances of the CERES radiation budget analysis over ERBE is the ability to use high spectral and spatial resolution cloud imager data to determine cloud and surface properties within the relatively large CERES field of view (20-km diameter for EOS-AM and EOS-PM, 10-km diameter for TRMM). For the first launch of the CERES broadband radiometer on TRMM in 1997, CERES will use the VIRS (Visible Infrared Scanner) cloud imager as input. For the next launches on EOS-AM (1998) and EOS-PM (2000), CERES will use the MODIS (Moderate-Resolution Imaging Spectroradiometer) cloud imager data as input. This subsystem matches imager-derived cloud properties with each CERES FOV and then uses either ERBE ADM's (Releases 1, 2, and 3) or improved CERES ADM's (Release 4) to derive TOA flux estimates for each CERES FOV. Until new CERES ADM's are available 3 years after launch, the primary advance over the ERBE TOA flux method will be to greatly increase the accuracy of the clear-sky fluxes. The limitations of ERBE clear-sky determination cause the largest uncertainty in estimates of cloud radiative forcing. In Release 4 using new ADM's, both rms and bias TOA flux errors for all scenes are expected to be a factor of 3-4 smaller than those for the ERBE-like analysis.

In addition to improved TOA fluxes, this subsystem also provides the CERES FOV matched cloud properties used by subsystem 5 to calculate radiative fluxes at the surface, within the atmosphere, and at the TOA for each CERES FOV. Finally, this subsystem also provides estimates of surface fluxes using direct TOA-to-surface parameterizations. Because of its complexity, this subsystem has been further decomposed into six additional subsystems.

4.1. Imager clear-sky determination and cloud detection. This subsystem is an extension of the ISCCP time-history approach with several key improvements, including the use of

- Multispectral clear/cloud tests (Gustafson 1994)
- Improved navigation (approximately 1 km or better) and calibration of VIRS and MODIS

4.2. Imager cloud height determination. For ISCCP, this step is part of the cloud property determination. CERES separates this step and uses three techniques to search for well-defined cloud layers:

- Comparisons of multispectral histogram analyses to theoretical calculations (Minnis et al. 1993)
- Spatial coherence (Coakley and Bretherton 1982)
- Infrared sounder radiance ratioing (15- μm band channels) (Menzel et al. 1992; Baum et al. 1994)

While the analysis of multilevel clouds is at an early development stage, it is considered a critical area and will be examined even in Release 2 of the CERES algorithms. The need for identification of multi-layer clouds arises from the sensitivity of surface downward LW flux to low-level clouds and cloud overlap assumptions (ATBD subsystem 5.0). Release 2 will attempt to determine which imager pixels

contain overlapped clouds. Later releases will examine the potential to derive multiple cloud layers (see Subsystem 4.0)

4.3. Cloud optical property retrieval. For ISCCP, this step involved the determination of a cloud optical depth using visible channel reflectance; an infrared emittance derived using this visible optical depth and an assumption of cloud microphysics (10- μm water spheres); and a cloud radiating temperature corrected for emittance less than 1.0 (daytime only). Version 2 (DX and D1) of the ISCCP analyses now becoming available allow for ice particles, depending on cloud temperature.

The CERES analysis extends these properties to include cloud particle size and phase estimation using additional spectral channels at 1.6 and 3.7 μm (TRMM) or 1.6 and 2.1 μm (MODIS) during the day (King et al. 1992) and 3.7 and 8.5 μm at night. In addition, the use of infrared sounder channels in subsystem 4.2 allows correction of non-black cirrus cloud heights for day and nighttime conditions.

Figure 4 summarizes the CERES cloud property analysis with a schematic drawing showing the cloud imager pixel data overlaid with a geographic mask (surface type and elevation), the cloud mask from subsystem 4.1, the cloud height and overlap conditions specified in subsystem 4.2, and the column of cloud properties for each imager pixel in the analysis region.

4.4. Convolution of imager cloud properties with CERES footprint point spread function. For each CERES FOV, the CERES point spread function (fig. 5) is used to weight the individual cloud imager footprint data to provide cloud properties matched in space and time to the CERES flux measurements. Because cloud radiative properties are non-linearly related to cloud optical depth, a frequency distribution of cloud optical depth is kept for each cloud height category in the CERES FOV. Additional information on cloud property data structures can be found in ATBD subsystem 0 and 4.0.

4.5. CERES inversion to instantaneous TOA fluxes. The cloud properties determined for each CERES FOV are used to select an ADM class to convert measured broadband radiance into an estimate of TOA radiative flux. In Releases 1 and 2, the ERBE ADM classes will be used. After several years of CERES RAP scanner data have been obtained, new ADM's will be developed as a function of cloud amount, cloud height, cloud optical depth, and cloud particle phase.

4.6. Empirical estimates of shortwave and longwave surface radiation budget involving CERES measurements. This subsystem uses parameterizations to directly relate the CERES TOA fluxes to surface fluxes. There are three primary advantages to using parameterizations:

- Can be directly verified against surface measurements
- Maximizes the use of the CERES calibrated TOA fluxes
- Computationally simple and efficient

There are two primary disadvantages to this approach:

- Difficult to obtain sufficient surface data to verify direct parameterizations under all cloud, surface, and atmosphere conditions
- May not be able to estimate all individual surface components with sufficient accuracy

For Release 2, we have identified parameterizations to derive surface net SW radiation (Cess et al. 1991; Li et al. 1993), clear-sky downward LW flux (ATBD subsystem 4.6.2), and total-sky downward LW flux (Gupta 1989; Gupta et al. 1992). Recent studies (Ramanathan et al. 1995; Cess et al. 1995) have questioned the applicability of the Li et al. 1993 surface SW flux algorithm, but this algorithm will be used in Release 2, pending the results of further validation.

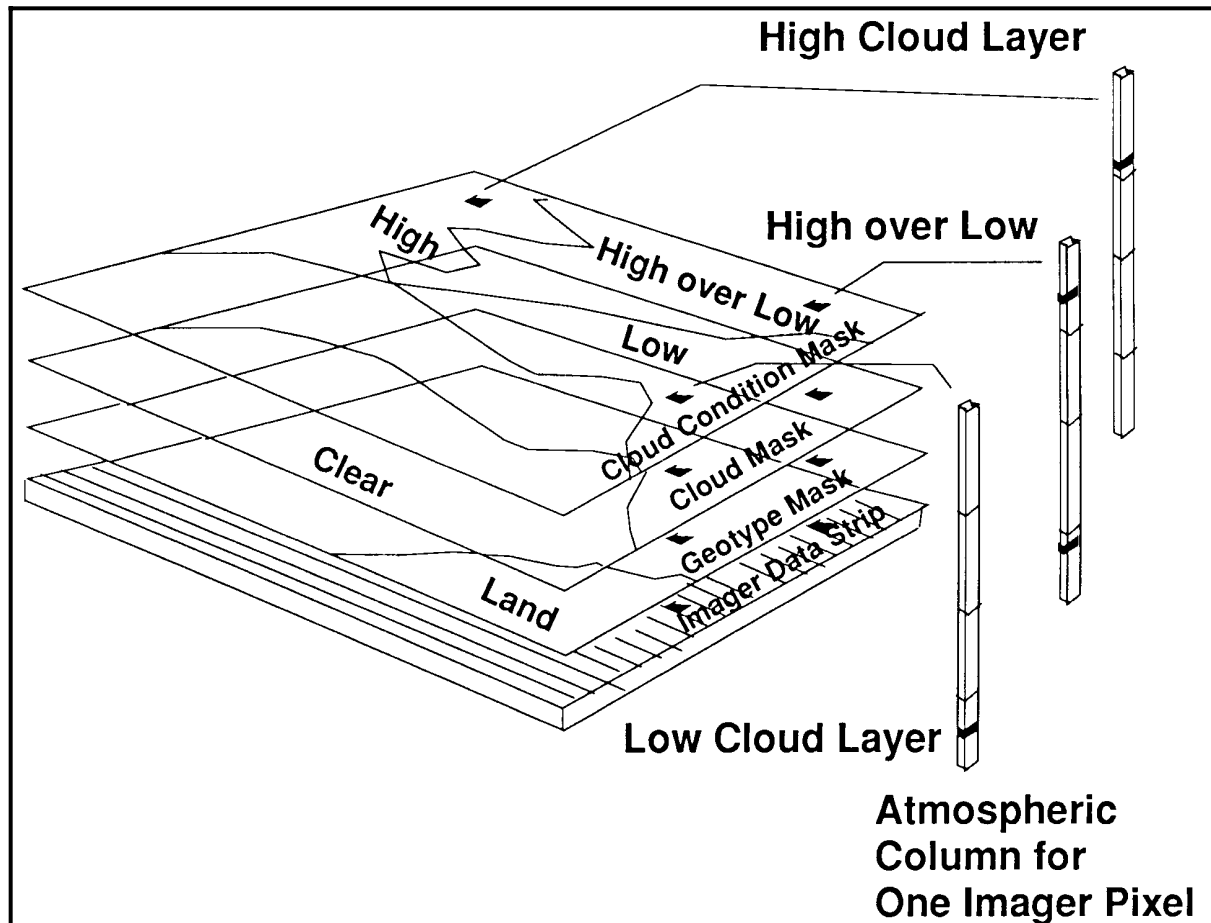


Figure 4. Illustration of the CERES cloud algorithm using cloud imager data from VIRS and MODIS. Imager data are overlaid by a geographic scene map, cloud mask, and cloud overlap condition mask. For each imager field of view, cloud properties are determined for one cloud layer (Release 2) or up to two cloud layers (Releases 3, 4).

The combined importance and difficulty of deriving surface fluxes has led CERES to a two fold approach. The results using the parameterizations given in subsystem 4.6 are saved in the CERES Surface Product. A separate approach using the imager cloud properties, radiative models, and TOA fluxes is summarized in subsystem 5.0 and these surface fluxes are saved in the CERES Atmosphere Products. Both approaches (subsystem 5.0 and 4.6) use radiative modeling to varying degrees. The difference is that the radiative models in the Surface Product are used to derive the form of a simplified parameterization between satellite observations and surface radiative fluxes. The satellite observations are primarily CERES TOA fluxes but include selected auxiliary observations such as column water vapor amount. These simplified surface flux parameterizations are then tested against surface radiative flux observations. If necessary, the coefficients of the parameterization are adjusted to obtain the optimal consistency with the surface observations.

Ultimately, the goal is to improve the radiative modeling and physical understanding to the point where they are more accurate than the simple parameterizations used in the Surface Product. In the near-term, validation against surface observations of both methods (subsystem 4.6 and 5.0) will be used to determine the most accurate approach. If the simplified surface flux parameterizations prove more accurate, then the surface fluxes derived in subsystem 4.6 will also be used as a constraint on the calculations of in-atmosphere fluxes derived in subsystem 5.0. This would probably be a weaker constraint than TOA fluxes, given the larger expected errors for surface flux estimates.

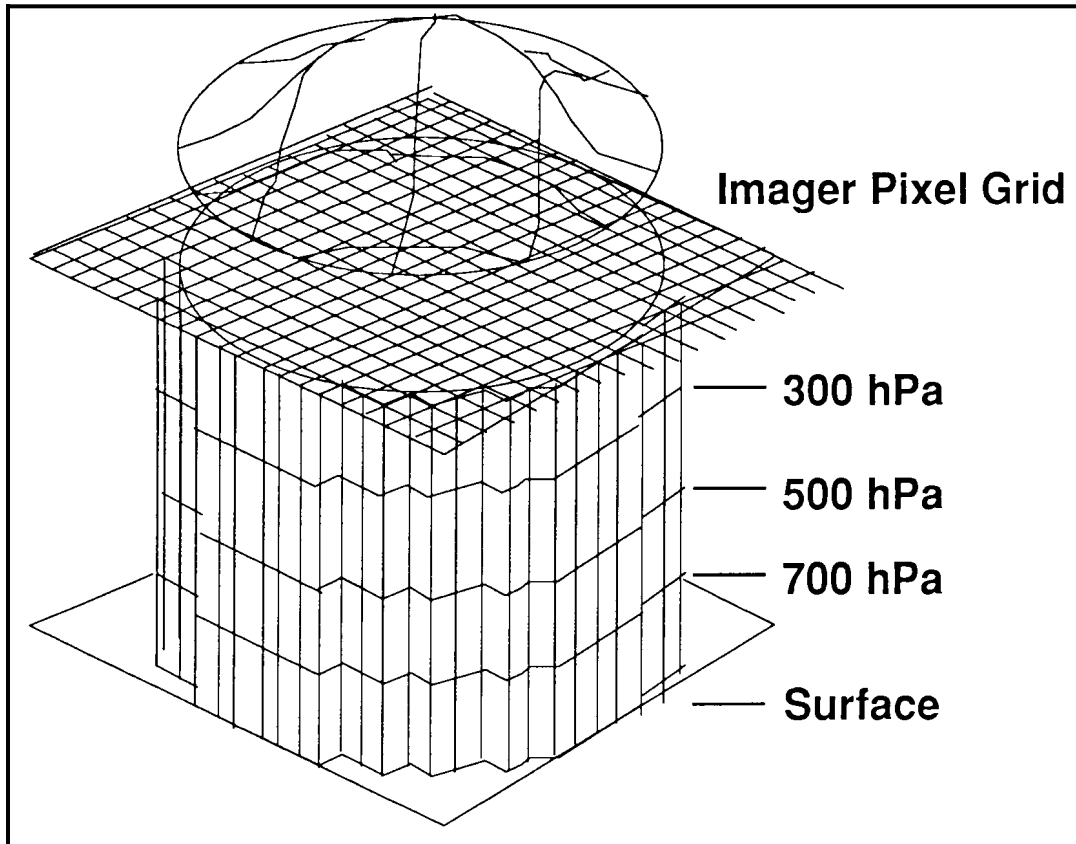


Figure 5. Illustration of the Gaussian-like point spread function for a single CERES field of view, overlaid over a grid of cloud imager pixel data. The four vertical layers represent the CERES cloud height categories which are separated at 700 hPa, 500 hPa, and 300 hPa. Cloud properties are weighted by the point spread function to match cloud and radiative flux data.

Subsystem 5: Compute Surface and Atmospheric Fluxes (ATMOSPHERE Data Product)

This subsystem is commonly known as SARB (Surface and Atmospheric Radiation Budget) and uses an alternate approach to obtain surface radiative fluxes, as well as obtaining estimates of radiative fluxes at predefined levels within the atmosphere. All SARB fluxes include SW and LW fluxes for both up and down components at all defined output levels from the surface to the TOA. For Release 2 (shown in fig. 1), output levels are the surface, 500 hPa, tropopause, and TOA. The major steps in the SARB algorithm for each CERES FOV are

1. Input surface data (albedo, emissivity)
2. Input meteorological data (T, q, O₃, aerosol)
3. Input imager cloud properties matched to CERES FOV's
4. Use radiative model to calculate radiative fluxes from observed properties
5. Adjust surface and atmospheric parameters (cloud, precipitable water) to get consistency with CERES observed TOA SW and LW fluxes; constrain parameters to achieve consistency with subsystem 4.6 surface flux estimates if validation studies show these surface fluxes to be more accurate than radiative model computations of surface fluxes
6. Save final flux calculations, initial TOA discrepancies, and surface/atmosphere property adjustments along with original surface and cloud properties

While global TOA fluxes have been estimated from satellites for more than 20 years, credible, global estimates for surface and in-atmosphere fluxes have only been produced globally in the last few

years (Darnell et al. 1992; Pinker and Laszlo 1992; Wu and Chang 1992; Charlock et al. 1993; Stuhlmann et al. 1993; Li et al. 1993; Gupta et al. 1992). Key outstanding issues for SARB calculations include

- Cloud layer overlap (see ATBD subsystem 5.0).
- Effect of cloud inhomogeneity (Cahalan et al. 1994).
- 3-D cloud effects (Schmetz 1984; Hiedinger and Cox 1994).
- Potential enhanced cloud absorption (Stephens and Tsay 1990; Cess et al. 1995; Ramanathan et al. 1995).
- Land surface bidirectional reflection functions, emissivity, and surface skin temperature (see ATBD subsystem 5.0).

For Release 2, SARB will use plane-parallel radiative model calculations and will treat cloud inhomogeneity by performing separate radiative computations for up to two non-overlapped cloud layers in each CERES fov. The average CERES fov optical depth for each cloud layer is defined by averaging the logarithm of imager pixel optical depth values, using the assumption that albedo varies more linearly with the logarithm of optical depth (Rossow et al. 1991).

For Release 2, adjustment of the calculated fluxes to consistency with the CERES instantaneous TOA fluxes can then be thought of as providing an “equivalent plane-parallel” cloud. For example, consider a fair weather cumulus field over Brazil viewed from the EOS CERES and MODIS instruments. Because the CERES ADM’s are developed as empirical models which are a function of cloud amount, cloud height, and cloud optical depth, the CERES radiative flux estimates can implicitly include 3-D cloud effects and in principle can produce unbiased TOA flux estimates. Note that this would not be true if CERES had inverted radiance to flux using plane-parallel theoretical models. The cloud optical depth derived from MODIS data, however, has been derived using a plane-parallel retrieval. If this imager optical depth is in error because of 3-D cloud effects, then the calculated SARB TOA SW flux will be in error and the cloud optical depth will be adjusted to compensate, thereby achieving a plane-parallel cloud optical depth which gives the same reflected flux as the 3-D cloud. In the LW, the cloud height might be adjusted to remove 3-D artifacts.

Tests against measured surface fluxes will be required to verify if these adjustments can consistently adjust surface fluxes as well; these comparisons have begun using the ARM Oklahoma Intensive Observing Periods (IOPs) in a joint CERES/ARM/GEWEX effort called CAGEX (Subsystem 5.0). Initial results are available on the World Wide Web. The data products from the SARB calculations will include both the magnitude of the required surface and cloud property adjustments, as well as the initial and final differences between calculated and TOA measured fluxes.

Figure 6 shows an example calculation of surface and atmospheric radiative fluxes both before and after adjustment to match TOA observations using ERBE. For Releases 1 and 2, we will test this approach using AVHRR and HIRS data to derive cloud properties, and ERBE TOA flux data to constrain the calculations at the TOA.

Subsystem 6: Grid Single Satellite Fluxes and Clouds and Compute Spatial Averages (ATMOSPHERE Data Product)

The next step in the processing of the CERES Atmosphere Data Products is to grid the output data from subsystem 5.0 into the EOS standard 1 degree equal angle grid boxes. The grid was chosen by EOS to simplify comparisons to global land, ocean, and atmosphere models. At high latitudes, where the distance between longitudinal steps become smaller, CERES will increase the longitude steps by factors of 2 to maintain consistent accuracy in the gridding process. Cloud properties and TOA fluxes from subsystem 4 and the additional surface and atmospheric radiative fluxes added in subsystem 5 are weighted by their respective area coverage in each grid box.

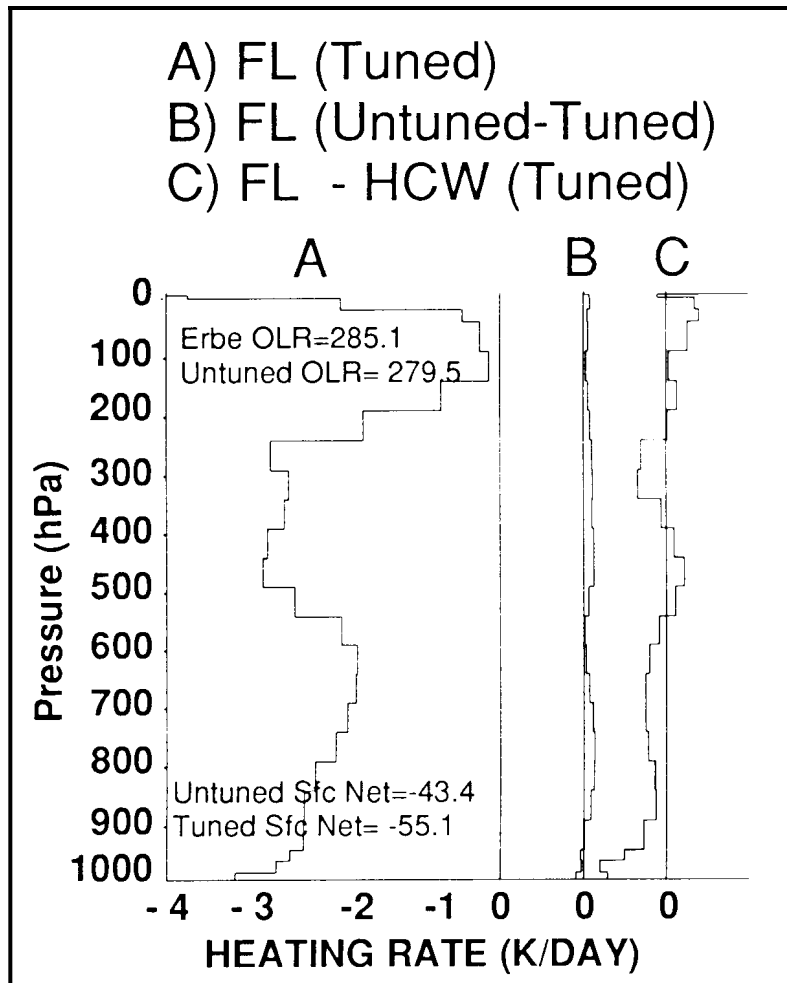


Figure 6. Test analysis of a clear-sky ERBE field of view over ocean using NMC temperature and water vapor. Initial calculation of TOA LW flux is in error by 5.6 Wm^{-2} , and the water vapor amount is tuned to match the TOA value. Curve A shows the tuned LW heating rate profile (degrees/day). Curve B shows the difference between tuned and untuned heating rates. Curve C shows the difference between the calculations of two different radiative transfer models. (See ATBD subsystem 5.0 for details.)

While spatial averaging of radiative fluxes (surface, in-atmosphere, and TOA) is relatively straightforward, spatial averaging of cloud properties is not so straightforward. The issue is most obvious when we consider the following thought experiment. We compare monthly average LW TOA fluxes in the tropical Pacific Ocean for June of 2 years, one of which was during an ENSO (El Niño/Southern Oscillation) event. We find a large change in TOA LW flux and want to know what change in cloud properties caused the change: cloud amount, cloud height, or cloud optical depth? Because cloud properties are nonlinearly related to radiative fluxes and we have simply averaged over all of those nonlinear relationships, we cannot guarantee that the question has an unambiguous answer. For example, consider that for TOA LW flux, changes in high cloud amount or optical depth have a large effect on LW flux. For low clouds, they have almost no effect. On the other hand, cloud height changes of either low or high clouds will have a roughly similar effect. Note that if we had selected a change in surface LW flux, the low clouds would dominate and the high clouds would have little effect. These are exactly the type of changes we need to examine and understand in order to address issues of cloud/climate feedback.

If we carry this analogy further, we can see that it is important to consider cloud changes at least as a function of five basic parameters:

- LW TOA flux
- LW surface flux
- SW TOA or surface flux (these are probably similar)
- Liquid water volume
- Ice water volume

The first three of these parameters are critical to cloud radiative forcing issues and the last two are critical to cloud dynamical modeling. We could also add in-atmosphere LW and SW net fluxes, but the five above are a good start. While the CERES team has not yet resolved the optimal way to address this issue, it has included in the data structures the capability to experiment in Release 2 with various formulations.

Subsystem 7: Time Interpolation and Synoptic Flux Computation for Single and Multiple Satellites (ATMOSPHERE Data Product)

Starting in November 1997, CERES will have one processing satellite (TRMM) sampling twice per day from 45°S to 45°N. In June 1998, the EOS-AM platform (10:30 a.m.; sun-synchronous) will increase diurnal sampling to 4 times per day. In 2000, the EOS-PM satellite (1:30 p.m.; sun-synchronous) will be launched. If TRMM is still functioning, or when a TRMM follow-on is launched CERES will then have 6 samples per day. Simulation studies using hourly GOES data indicate that the ERBE time-space averaging algorithm gives regional monthly mean time sampling errors (1σ) which are about:

- 9 $W\cdot m^{-2}$ for TRMM alone
- 4 $W\cdot m^{-2}$ for TRMM plus EOS AM
- 2 $W\cdot m^{-2}$ for TRMM plus EOS AM plus EOS PM

Since satellites can fail prematurely, it is very useful to provide a strategy to reduce time sampling errors, especially for the single satellite case.

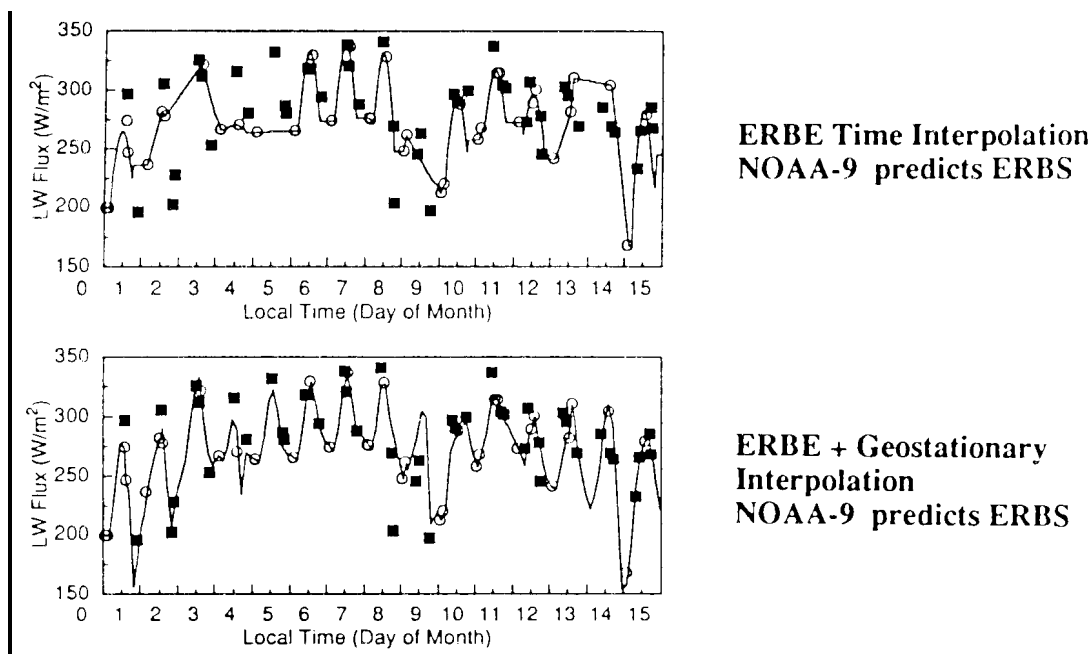


Figure 7. Time Series of ERBE ERBS (solid squares) and NOAA-9 (open circles) LW flux observations and interpolated values from July 1985 over New Mexico. The top curve shows the ERBE time interpolated values; bottom curve the geostationary-data-enhanced interpolation.

The CERES strategy is to incorporate 3-hourly geostationary radiance data to provide a correction for diurnal cycles which are insufficiently sampled by CERES. The key to this strategy is to use the geostationary data to supplement the shape of the diurnal cycle, but then use the CERES observations as the absolute reference to anchor the more poorly-calibrated geostationary data. One advantage of this method is that it produces 3-hourly synoptic radiation fields for use in global model testing, and for improved examination of diurnal cycles of clouds and radiation. The output of subsystem 7 is an estimate of cloud properties and surface, atmosphere, and TOA fluxes at each 3-hourly synoptic time. These estimates are also used later in subsystem 8 to aid in the production of monthly average cloud and radiation data.

The process for synoptic processing involves the following steps:

1. Regionally and temporally sort and merge the gridded cloud and radiation data produced by subsystem 6
2. Regionally and temporally sort and merge the near-synoptic geostationary data
3. Interpolate cloud properties from the CERES times of observation to the synoptic times
4. Interpolate cloud information and angular model class, convert the narrowband GOES radiance to broadband (using regional correlations to CERES observations), and then convert the broadband radiance to broadband TOA flux (using the CERES broadband ADM's)
5. Use the time-interpolated cloud properties to calculate radiative flux profiles as in subsystem 5, using the synoptic TOA flux estimates as a constraint
6. Use the diurnal shape of the radiation fields derived from geostationary data, but adjust this shape to match the CERES times of observations (assumed gain error in geostationary data)

Figure 7 gives an example of the enhanced time interpolation using geostationary data.

The system described above could also use the ISCCP geostationary cloud properties. The disadvantage of this approach is that it incorporates cloud properties which are systematically different and less accurate than those from the cloud imagers flying with CERES. The ISCCP cloud properties are limited by geostationary spatial resolution, spectral channels, and calibration accuracy. In this sense, it would be necessary to "calibrate" the ISCCP cloud properties against the TRMM and EOS cloud properties. We are currently performing sensitivity studies on the utility of the ISCCP cloud properties for this purpose.

Subsystem 8: Monthly Regional, Zonal, and Global Radiation Fluxes and Cloud Properties (ATMOSPHERE Data Product)

This subsystem uses the CERES instantaneous synoptic radiative flux and cloud data (subsystem 7) and time averages to produce monthly averages at regional, zonal, and global spatial scales. Initial simulations using both 1-hourly and 3-hourly data have shown that simple averaging of the 3-hourly results is adequate for calculating monthly average LW fluxes. SW flux averaging, however, is more problematic. The magnitude of the solar flux diurnal cycle is 10 to 100 times larger than that for LW flux.

Two methods for SW time averaging are currently being tested using Release 2 data. The first method uses the same techniques as subsystem 7, but to produce 1-hourly instead of 3-hourly synoptic maps. Time averaging then proceeds from the 1-hourly synoptic fields. The second method starts from the 3-hourly synoptic data, and then time interpolates using methods similar to ERBE (Brooks et al. 1986) for other hours of the day with significant solar illumination. While the use of models of the solar zenith angle dependence of albedo are adequate for TOA and surface fluxes, we will examine extensions of these techniques to include interpolation of solar absorption within the atmospheric column. A key issue is to avoid biases caused by the systematic increase of albedo with solar zenith angle for times of observation between sunset and sunrise and the first daytime observation hour.

Subsystem 9: Grid TOA and Surface Fluxes for Instantaneous Surface Product (SURFACE Data Product)

This subsystem is essentially the same process as in subsystem 6. The major difference is that instead of gridding data to be used in the Atmosphere Data Products (subsystems 5, 6, 7, and 8), this subsystem spatially grids the data to be used in the Surface Data Products (subsystems 9 and 10). The spatial grid is the same: 1.0 degree equal angle. See the data flow diagram (figure 2) and the associated discussion for a summary of the difference between the Atmosphere and Surface Data Products.

Subsystem 10: Monthly Regional TOA and Surface Radiation Budget (SURFACE Data Product)

The time averaging for the Surface Data Product is produced by two methods. The first method is the same as the ERBE method (ERBE-like product in subsystem 3) with the following exceptions:

- Improved CERES models of solar zenith angle dependence of albedo
- Improved cloud imager scene identification (subsystem 4) and improved CERES ADM's to provide more accurate instantaneous fluxes
- Simulation studies indicate that the monthly averaged fluxes will be a factor of 2-3 more accurate than the ERBE-like fluxes

The second method incorporates geostationary radiances similar to the process outlined for synoptic products in subsystem 7. We include this method to minimize problems during the initial flight with TRMM when we have only one spacecraft with two samples per day. As the number of satellites increases to 3, the geostationary data will have little impact on the results.

Because one of the major rationales for the Surface Data Products is to keep surface flux estimates as closely tied to the CERES direct observations as possible, this subsystem will not calculate in-atmosphere fluxes, and will derive its estimates of surface fluxes by the same methods discussed in subsystem 4.6.

Subsystem 11: Grid Geostationary Narrowband Radiances

CERES will use 3-hourly geostationary radiance data to assist diurnal modeling of TOA fluxes and to minimize temporal interpolation errors in CERES monthly mean TOA flux products. This subsystem is essentially the same process as in subsystem 6. The major difference is that the process is performed on geostationary radiances instead of CERES TOA fluxes. The current input data are one month of 3-hourly ISCCP B1 geostationary (GEO) data which contain visible (VIS) and infrared (IR) narrowband radiances from different satellites. At the present time, GEO data are available for four satellites; METEOSAT, GOES-East, GOES-West, and GMS. The spatial resolution of the GEO data set is approximately 10 km. These data are gridded and spatially averaged into CERES 1-degree equal-angle grid boxes using functions described in subsystem 6. The outputs consist of mean and statistics of VIS and IR narrowband radiances for each of the CERES 1-degree grid box and each of the 3-hourly synoptic time. This data product represents a major input source for both subsystem 7 and 10.

Subsystem 12: Regrid Humidity and Temperature Fields

This subsystem describes interpolation procedures used to convert temperature, water vapor, ozone, aerosols, and passive microwave column water vapor obtained from diverse sources to the spatial and temporal resolution required by various CERES subsystems. Most of the inputs come from EOS DAO or NOAA NCEP analysis products, although the subsystem accepts the inputs from many different sources on many different grids. The outputs consist of the same meteorological fields as the inputs, but at a uniform spatial and temporal resolution necessary to meet the requirements of the other CERES processing subsystems. Interpolation methods vary depending on the nature of the field. For Release 2, CERES is planning to use the DAO analysis products. One of the key issues for use of analysis products

in a climate data set is the “freezing” of the analysis product algorithms during the climate record. DAO has agreed to provide a consistent analysis method for CERES.

Relationships to Other EOS Instruments and non-EOS Field Experiments: Algorithm Validation and Interdisciplinary Studies

While the ties to VIRS on TRMM and MODIS on EOS have been obvious throughout this overview, there are ties between the CERES data products and many of the EOS instruments.

We expect to greatly increase our ability to detect cloud overlap by using the passive microwave retrievals of cloud liquid water path from the TMI (TRMM Microwave Imager), as well as the AMSR (Advanced Microwave Scanning Radiometer) instrument on EOS-PM (2000) and MIMR (Multifrequency Imaging Microwave Radiometer) on METOP (Meteorological Operational Polar Platform). METOP (2000) is the European morning sun-synchronous satellite which will provide passive microwave data in the same orbit as the EOS-AM platform. This constellation of instruments will allow a 3-satellite system with CERES/cloud imager/passive microwave instruments on each spacecraft. This suite provides both adequate diurnal coverage as well as greatly increased ability to detect the presence of multi-layer clouds, even beneath a thick cirrus shield. Passive microwave liquid water path will be tested using TRMM data for multilayer clouds over ocean and may be included for Release 4.

The MISR (Multiangle Imaging Spectroradiometer) and ASTER (Advanced Spaceborne Thermal Emission and Reflection Radiometer) onboard the EOS-AM platform will provide key validation data for the CERES experiment. MISR can view 300-km wide targets on the earth nearly simultaneously (within 10 minutes) from 9 viewing zenith angles using 9 separate CCD (charged coupled device) array cameras. This capability provides independent verification of CERES bidirectional reflectance models, as well as stereo cloud height observations. For broadband radiative fluxes, MISR has better angular sampling than CERES, but at the price of poorer time and spectral information (narrowband instead of broadband). The POLDER (Polarization of Directionality of Earth's Reflectances) instrument launched on the ADEOS (Advanced Earth Observing System) platform in 1996 will also allow tests of CERES anisotropic models using narrowband models. ASTER on the EOS-AM platform will provide Landsat-like very high spatial resolution data to test the effect of MODIS and VIRS coarser resolution data (i.e., beam filling problems) on the derivation of cloud properties.

In September 1994, the LITE (Lidar In-Space Technology Experiment) provided the first high-quality global lidar observations of cloud height from space. These data will be a key source determine the spatial scale of cloud height variations around the globe. Unfortunately, the limited duty cycle of lidar data collection during the 2-week Space Shuttle mission resulted in only a few coincidences with GOES, SSM/I, or NOAA polar orbiting spacecraft. Nevertheless, the limited data available showed that unlike aircraft or surface based lidar, the space-based lidar could penetrate to the top of boundary layer cloud or to the surface of the Earth at least 75% of the time. This effect is due to additional forward scattered photons which remain within the relatively large space-based lidar field of view of 300 meters.

Given the relative importance of multi-layered cloud to calculations of longwave surface and atmospheric radiative fluxes, clearly a space-based cloud lidar and/or radar mission is essential in the future. Recent studies in support of NASA's new ESSP (Earth System Science Pathfinder) program indicate that the ideal combination to resolve all multi-layered cloud is a lidar for optically thin and physically thin cloud layers, combined with a cloud radar (3 mm or 8 mm) for optically and physically thick layers. Space-based cloud lidar can resolve thin clouds to 50 m vertical resolution, while cloud radar has a vertical resolution of about 500 m. At the same time, a cloud radar will be able to observe optically thick layers (visible optical thickness greater than about 10) which will attenuate the lidar signal. A combined lidar/radar mission which synchronized its orbit with the EOS-AM or PM would be ideal for global validation of CERES and EOS cloud properties, including the difficult polar cloud cases.

Spaceborne cloud radar has been endorsed as a high priority mission by the GEWEX (Global Energy and Water Cycle Experiment) of the World Climate Research Program).

The GLAS (Geoscience Laser Altimetry System) planned for launch in 2002 may include cloud lidar capability, but the orbit optimization required for its primary mission (i.e. measuring ice sheet volume), is not very effective for validation of EOS cloud properties. As currently planned, GLAS will obtain about 1% of its data (approximately 10% of 1 month each year) nearly simultaneous with EOS-AM, depending on the final selected orbit altitude.

Established surface sites (i.e. ARM, BSRN, SURFMAP) will provide one of the most critical sources of validation for CERES surface radiative fluxes and cloud properties. The 3 ARM sites in Oklahoma, the western tropical Pacific Ocean, and the North Slope of Alaska will provide the most critical long-term time series of validation data. These sites will include measurements of SW and LW surface fluxes, cloud lidar, cloud radar, microwave liquid water path, and newly developing estimates of the vertical profiles of cloud microphysics in both water and ice cloud layers. For surface fluxes, the BSRN sites will provide additional sites for carefully calibrated and maintained SW and LW surface fluxes. The major limitation of these sites will be the lack of observations in other important climatic regimes (i.e. desert, midlatitude ocean, tropical land, subtropical ocean, and heavily vegetated midlatitude land).

Finally, field experiment campaigns will be necessary to extend the climatological regimes sampled by the ARM and BSRN sites. These campaigns will require coordination of surface and in-situ aircraft cloud and radiation data during overpasses of the EOS spacecraft. CERES science team members are active participants on the FIRE, ARM, and GEWEX GCIP experiment teams. CERES will rely on these national and international programs to provide critical validation data. It is expected that the accuracy of CERES validation efforts will systematically improve as additional surface/satellite and field experiment/satellite coincidences are obtained. A large number of such coincidences will be required in order to validate the wide range of cloud and climate conditions within the global climate system. Validation plan drafts have been prepared for each of the CERES data products and were reviewed in Fall, 1996. The plans should be revised and available on the same World Wide Web site as the CERES ATBDs by August 1997.

References

- Barkstrom, B. R. 1984: The Earth Radiation Budget Experiment (ERBE). *Bull. Am. Meteorol. Soc.*, vol. 65, pp. 1170–1185.
- Barkstrom, B. R.; and Smith, G. L. 1986: The Earth Radiation Budget Experiment: Science and Implementation. *Rev. Geophys.*, vol. 24, pp. 379–390.
- Baum, Bryan A.; Arduini, Robert F.; Wielicki, Bruce A.; Minnis, Patrick; and Si-Chee, Tsay 1994: Multilevel Cloud Retrieval Using Multispectral HIRS and AVHRR Data: Nighttime Oceanic Analysis. *J. Geophys. Res.*, vol. 99, no. D3, pp. 5499–5514.
- Brooks, D. R.; Harrison, E. F.; Minnis, P.; Suttles, J. T.; and Kandel, R. S. 1986: Development of algorithms for Understanding the Temporal and Spatial Variability of the Earth's Radiation Balance. *Rev. Geophys.*, vol. 24, pp. 422–438.
- Cahalan, Robert F.; Ridgway, William; Wiscombe, Warren J.; Gollmer, Steven; and Harshvardhan 1994: Independent Pixel and Monte Carlo Estimates of Stratocumulus Albedo. *J. Atmos. Sci.*, vol. 51, no. 24, pp. 3776–3790.
- CEES 1994: Our Changing Planet. The FY 1994 U.S. Global Change Research Program. National Science Foundation, Washington, DC, p. 84.
- Cess, Robert D.; Jiang, Feng; Dutton, Ellsworth G.; and Deluisi, John J. 1991: Determining Surface Solar Absorption From Broadband Satellite Measurements for Clear Skies—Comparison With Surface Measurements. *J. Climat.*, vol. 4, pp. 236–247.
- Cess, R. D.; Zhang, M. H.; Minnis, P.; Corsetti, L.; Dutton, E. G.; Forgan, B. W.; Garber, D. P.; Gates, W. L.; Hack, J. J.; and Harrison, E. F. 1995: Absorption of Solar Radiation by Clouds: Observations Versus Models. *Science*, vol. 267, no. 5197, pp. 496–498.

- Charlock, T. P.; Rose, F. G.; Yang, S.-K.; Alberta, T.; and Smith, G. L. 1993: An Observational Study of the Interaction of Clouds, Radiation, and the General Circulation. *Proceedings of IRS 92: Current Problems in Atmospheric Radiation*, A. Deepak Publ., 151–154.
- Coakley, J. A., Jr.; and Bretherton, F. P. 1982: Cloud Cover From High-Resolution Scanner Data—Detecting and Allowing for Partially Filled Fields of View. *J. Geophys. Res.*, vol. 87, pp. 4917–4932.
- Darnell, Wayne L.; Staylor, W. Frank; Gupta, Shashi K.; Ritchey, Nancy A.; and Wilber, Anne C. 1992: Seasonal Variation of Surface Radiation Budget Derived From International Satellite Cloud Climatology Project C1 Data. *J. Geophys. Res.*, vol. 97, no. D14, pp. 15741–15760.
- Gupta, Shashi K. 1989: A Parameterization for Longwave Surface Radiation From Sun-Synchronous Satellite Data. *J. Climat.*, vol. 2, pp. 305–320.
- Gupta, Shashi K.; Darnell, Wayne L.; and Wilber, Anne C. 1992: A Parameterization for Longwave Surface Radiation From Satellite Data—Recent Improvements. *J. Appl. Meteorol.*, vol. 31, no. 12, pp. 1361–1367.
- Gustafson, G.B., et al. 1994: Support of environmental requirements for cloud analysis and archive (SERCAA): Algorithm descriptions. Phillips Laboratory, 29 Randolph Road, Hanscom AFB, MA 01731-3010, Report Number PL-TR-94-2114, 108 pp.
- Hansen, James; Lacis, Andrew; Ruedy, Reto; Sato, Makito; and Wilson, Helene 1993: How Sensitive is the World's Climate? *Natl. Geogr. Res. & Explor.*, vol. 9, no. 2, pp. 142–158.
- Hiedinger, A.; and Cox, S. 1994: Radiative Surface Forcing of Boundary Layer Clouds. *Eighth Conference on Atmospheric Radiation*, pp. 246–248.
- King, Michael D.; Kaufman, Yoram J.; Menzel, W. Paul; and Tanre, Didier D. 1992: Remote Sensing of Cloud, Aerosol, and Water Vapor Properties From the Moderate Resolution Imaging Spectrometer (MODIS). *IEEE Trans. Geosci. & Remote Sens.*, vol. 30, pp. 2–27.
- Lee, R. B.; Barkstrom, B. R.; Smith, G. L.; Cooper, J. E.; Kopia, L. P.; Lawrence, R. W. April 1996: The Clouds and the Earth's Radiant Energy System (CERES) Sensors and Preflight Calibration Plans. *Journal of Atmospheric and Oceanic Technology*, vol. 13, no.2.
- Li, Zhanqing; and Leighton, H. G. 1993: Global Climatologies of Solar Radiation Budgets at the Surface and in the Atmosphere From 5 Years of ERBE Data. *J. Geophys. Res.*, vol. 98, no. D3, pp. 4919–4930.
- Li, Zhanqing; Leighton, H. G.; Masuda, Kazuhiko; and Takashima, Tsutomu 1993: Estimation of SW Flux Absorbed at the Surface From TOA Reflected Flux—Top of Atmosphere. *J. Climat.*, vol. 6, no. 2, pp. 317–330.
- Menzel, W. P.; Wylie, D. P.; and Strabala, K. L. 1992: Seasonal and Diurnal Changes in Cirrus Clouds as Seen in Four Years of Observations With the VAS. *J. Appl. Meteorol.*, vol. 31, pp. 370–385.
- Minnis, Patrick; Kuo-Nan, Liou; and Young, D. F. 1993: Inference of Cirrus Cloud Properties Using Satellite-Observed Visible and Infrared Radiances. II—Verification of Theoretical Radiative Properties. *J. Atmos. Sci.*, vol. 50, pp. 1305–1322.
- Pinker, R. T.; and Laszlo, I. 1992: Modeling Surface Solar Irradiance for Satellite Applications on a Global Scale. *J. Appl. Meteorol.*, vol. 31, pp. 194–211.
- Ramanathan, V.; Subasilar, B.; Zhang, G. J.; Conant, W.; Cess, R. D.; Kiehl, J. T.; Grassl, H.; and Shi, L. 1995: Warm Pool Heat Budget and Shortwave Cloud Forcing—A Missing Physics? *Science*, vol. 267, pp. 499–503.
- Ramanathan, V.; Cess, R. D.; Harrison, E. F.; Minnis, P.; and Barkstrom, B. R. 1989: Cloud-Radiative Forcing and Climate—Results From the Earth Radiation Budget Experiment. *Science*, vol. 243, pp. 57–63.
- Randall, David A.; Harshvardhan; Dazlich, Donald A.; and Corsetti, Thomas G. 1989: Interactions Among Radiation, Convection, and Large-Scale Dynamics in a General Circulation Model. *J. Atmos. Sci.*, vol. 46, pp. 1943–1970.
- Rossow, W.; Garder, L.; Lu, P.; and Walker, A. 1991: International Satellite Cloud Climatology Project (ISCCP) Documentation of Cloud Data. In WMO/TD-No. 266 (Revised), *World Meteorol. Org.*, p. 76.
- Rossow, William B.; and Garder, Leonid C. 1993: Cloud Detection Using Satellite Measurements of Infrared and Visible Radiances for ISCCP. *J. Climat.*, vol. 6, no. 12, pp. 2341–2369.

- Schmetz, J. 1984: On the Parameterization of the Radiative Properties of Broken Clouds. *Tellus*, vol. 36A, pp. 417–432.
- Smith, G. Louis; Green, Richard N.; Raschke, Ehrhard; Avis, Lee M.; Suttles, John T.; Wielicki, Bruce A.; and Davies, Roger 1986: Inversion Methods for Satellite Studies of the Earth Radiation Budget: Development of Algorithms for the ERBE Mission. *Rev. Geophys.*, vol. 24, pp. 407–421.
- Stephens, Graeme L.; and Tsay, Si-Chee 1990: On the Cloud Absorption Anomaly. *R. Meteorol. Soc.*, vol. 116, pp. 671–704.
- Stowe, L. L.; McClain, E. P.; Carey, R.; Pellegrino, P.; and Gutman, G. G. 1991: Global Distribution of Cloud Cover Derived From NOAA/AVHRR Operational Satellite Data. *Adv. Space Res.*, vol. 11, no. 3, pp. 51–54.
- Stuhlmann, R.; Raschke, E.; and Schmid, U. 1993: *Cloud Generated Radiative Heating From METEOSAT Data. Proceedings of IRS 92: Current Problems in Atmospheric Radiation*. A. Deepak Publ., pp. 69–75.
- Suttles, John T.; Wielicki, Bruce A.; and Vemury, Sastri 1992: Top-of-Atmosphere Radiative Fluxes—Validation of ERBE Scanner Inversion Algorithm Using Nimbus-7 ERB Data. *J. Appl. Meteorol.*, vol. 31, no. 7, pp. 784–796.
- Welch, R. M.; Sengupta, S. K.; Goroch, A. K.; Rabindra, P.; Rangaraj, N.; and Navar, M. S. 1992: Polar Cloud and Surface Classification Using AVHRR Imagery—An Intercomparison of Methods. *J. Appl. Meteorol.*, vol. 31, no. 5, pp. 405–420.
- Wielicki, Bruce A.; and Green, Richard N. 1989: Cloud Identification for ERBE Radiative Flux Retrieval. *J. Appl. Meteorol.*, vol. 28, no. 11, pp. 1133–1146.
- Wielicki, Bruce A.; Cess, R. D.; King, M. D.; Randall, D. A.; Harrison, E. F. 1995: Mission to Planet Earth: Role of Clouds and Radiation in Climate. *Bull. Amer. Meteorol. Soc.*, vol. 76, pp. 2125–2153.
- Wu, Man L. C.; and Chang, Lang-Ping 1992: Longwave Radiation Budget Parameters Computed From ISCCP and HIRS2/MSU Products. *J. Geophys. Res.*, vol. 97, no. D9, pp. 10083–10101.
- Climate Change 1995: “The Science of Climate Change.” J. T. Houghton, L. G. Meira Filho, B. A. Callender, N. Harris, A. Kattenberg and K. Maskell (eds.). Cambridge University Press, UK. 572 pp. (ISBN: 0-521-56433-6)